Limitations of Monitoring Wells for the Detection and Quantification of Petroleum Products in Soils and Aquifers

by Abdul S. Abdul, Sheila F. Kia, and Thomas L. Gibson

Abstract

Theoretical analysis and laboratory column experiments were carried out to investigate the conditions required for petroleum products (oil) to flow into a well installed through a sandy porous medium contaminated with the oil. The results indicated that oil would flow into a well only after a layer of "free oil" is formed in the adjacent porous medium. Because significant quantities of oil could be stored in the porous medium under the influence of capillary suction prior to the formation of the zone of free oil, the presence of oil in a well would indicate an advanced stage of oil contamination of the subsurface. While monitoring wells could be used to delineate the extent of the free-oil plume and the plume of dissolved petroleum constituents, they are not useful for delineating the extent of capillary held oil.

The experimental results also indicated that the ratio of the oil-layer thickness in the well to that in the porous medium is not a constant as is sometimes assumed in practice. Further, estimates of the oil thickness in the medium based on the oil thickness in wells and on capillary properties measured in the laboratory were sensitive to the values of the parameters used in these estimates. The measured thickness of the oil layer in a monitoring well alone may not yield reliable estimates of the amount of oil in the subsurface, and assuming that the oil-thickness ratio is a constant can lead to inadequate site assessments and inappropriate remedial plans.

Introduction

Petroleum products, hereafter referred to as "oil," such as gasoline, diesel fuel, kerosene, transmission fluid, and lubricating oils, are commonly stored in underground storage tanks (USTs). It is widely known that USTs can develop leaks as a result of material failure or negligence. Such leaks are not only a costly loss of the petroleum product, but an environmental concern. In view of this, it is generally agreed that methods for the early detection of leaks and for the delineation of zones of contamination are needed, because they can serve to limit the adverse effects of products leaked from USTs.

Monitoring wells have proven to be very useful for detecting the presence of aqueous phase contaminants migrating from waste sites such as landfills and surface impoundments. Thus, it is not surprising that monitoring wells are frequently used for detecting leaks from USTs and for delineating the plumes of oil resulting from such leaks. Monitoring wells are useful for delineating the region of the aquifer contaminated with dissolved constituents of petroleum products; however, the appropriateness of monitoring wells to detect the presence and delineate the extent of undissolved petroleum products in soil and aquifer systems is questionable. These concerns are investigated in this study.

Theoretical Background

Detection and Delineation

A schematic of a cross section of the unsaturated-saturated subsurface zones, under conditions in which the water table is at such a depth below the ground that the surface soil has drained to residual saturation, is shown in Figure 1. Essentially, this figure illustrates the relationship between the degree of saturation and the fluid pressure above the water table. By this relationship, the fluid pressure (gauge) becomes more negative with height above the water table, where the fluid pressure is zero. Further, the degree of saturation is approximately constant in the capillary fringe (almost 100 percent saturation) and in the pendular zone (residual saturation), and it decreases with height above the water table in the funicular zone.

Fluids in the capillary fringe and funicular zone are held mainly by capillary forces and are, therefore, said to be under suction. Consider a capillary pore in a porous medium. The capillary pressure (p_c) that exists at the interface between two fluids in the pore is the difference between the pressures in the non-wetting (p_{nw}) and wetting (p_w) fluids (Equation 1 [Corey 1977]). The capillary pressure can also be described by Equation 2, while the fluid

pressure head (ψ) can be described by Equation 3 (Corey 1977).

$$p_c = p_{nw} - p_w \qquad (1)$$

$$p_c = \frac{2\sigma \cos \theta}{r_{eff}} \qquad (2)$$

$$\psi = h = -\frac{P_c}{(\rho_w - \rho_{nw})g} \qquad (3)$$

where,

p	$\equiv$	fluid pressure, (F/L^2)
nw	$\equiv$	non-wetting fluid
w	$\equiv$	wetting fluid
r_{eff}	$\equiv$	effective pore radius, (L)
σ	$\equiv$	interfacial tension, (F/L)
θ	$\equiv$	contact angle, (degree)
h	$\equiv$	capillary rise, (L)
ρ	$\equiv$	density, (M/L^3)
g	$\equiv$	gravitational constant
ψ	$\equiv$	pressure head, (L)

Based on principles of fluid mechanics, fluid would flow from zones of higher (or less negative) values of ψ to zones of lower values of ψ along the same horizontal plane. Monitoring wells are usually several inches in diameter; thus, they do not exert capillary forces. Therefore, the region above the liquid level in a well will be filled with air (zero-pressure head). In contrast, the pendular, funicular, and capillary fringe zones in contact with the air-filled portion of the well screen are made up of a network of capillaries and water or oil in these capillaries will be under negative-pressure head. Liquids from these zones being under negative-pressure head are not expected to flow from the porous medium into the well. If the well is installed below the water table or through a zone of free oil, where the pressure head of the liquid is greater than atmospheric pressure, liquid would flow into the well until, if there is no vertical hydraulic gradient, the liquid level in the well would rise to the same level as that in the porous medium.

Based on the concepts in Figure 1 and principles of fluid mechanics (Dullien 1979) the vertical profiles of oil saturation and pressure can be sketched for different stages of an oil-leak event. Figure 2 shows such profiles for three stages during an oil-leak event in a uniform sandy medium. In these examples, the rate of oil leak (volume/area) is smaller than the saturated oil hydraulic conductivity of the medium.

Figure 2a shows three stages of an oil leak. Stage 1 shows conditions soon after a leak started, when the oil is distributed only in the pendular and funicular zones. Oil spreading in these zones will be both lateral and downward under the influence of capillary and gravity forces, respectively (Corey 1977). In Stage 2, oil has migrated into the water capillary fringe and an oil capillary fringe has developed, but free oil is not present. The lateral spread of the oil in the water capillary fringe zone is in the direction of ground water flow. Stage 3 represents an advanced stage of the oil leak, when an "oil table" has developed. The actual position of the oil table will depend
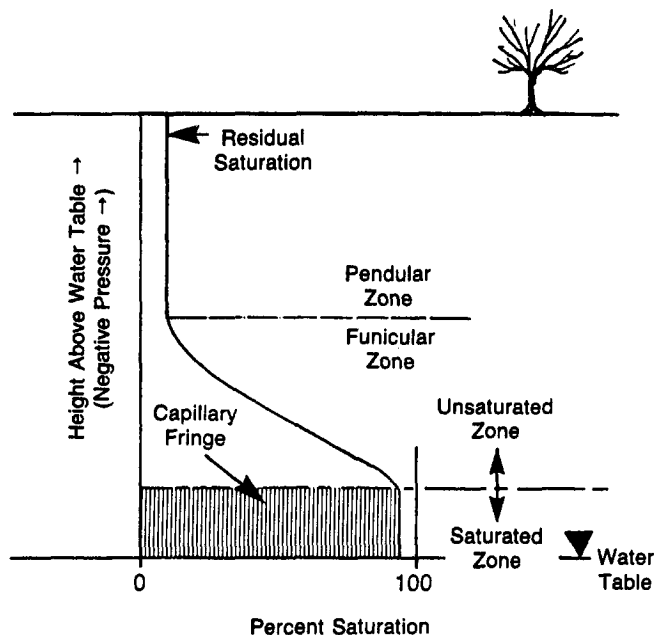

Figure 1. Schematic of the unsaturated and saturated subsurface zones.

on the rate of leak, the quantity of oil, the properties of the oil, and the properties of the hydrogeologic material.

Figure 2b shows the degree of saturation profiles of oil along a vertical line through each of the three stages. Before the oil leak, the medium was variably saturated with water, with the degree of water saturation increasing with depth through the funicular zone. In Stage 1 soon after the leak starts, the oil saturation is expected to be greatest near the leak and to decrease with depth into the medium below the leak. In Stage 2, oil has started to accumulate within the water capillary fringe because the oil head is not large enough to further displace the pore water downward (Equation 2). At this stage of the leak, an extensive region of the subsurface could become contaminated and a large volume of oil could be stored as residual and capillary-held oil within the medium. However, because the oil pressure is still negative, the oil should not flow into a well. In Stage 3, the region of oil saturation has increased to form a zone of "free oil." This free oil will be at a higher pressure than atmospheric and could flow into a well open to the zone of free oil.

Figure 2c shows the expected vertical oil-pressure distributions for the three stages of an oil leak. The oil-pressure distribution follows that of the degree of saturation, by which the values of pressure head decrease downward from the source during Stage 1 and the trend reverses for Stages 2 and 3. The oil-pressure head during Stages 1 and 2 is negative (below atmospheric pressure), while it is positive in the zone of free oil, which develops during Stage 3. As discussed previously, fluid would only flow from high to low pressure head along the same horizontal plane. Therefore, oil in the pendular, funicular, and capillary fringe zones being under negative pressure, would not flow directly into a well.

Based on this theoretical analysis, considerable oil contamination can occur without oil flowing into wells. A main task in this study was to carry out experiments to
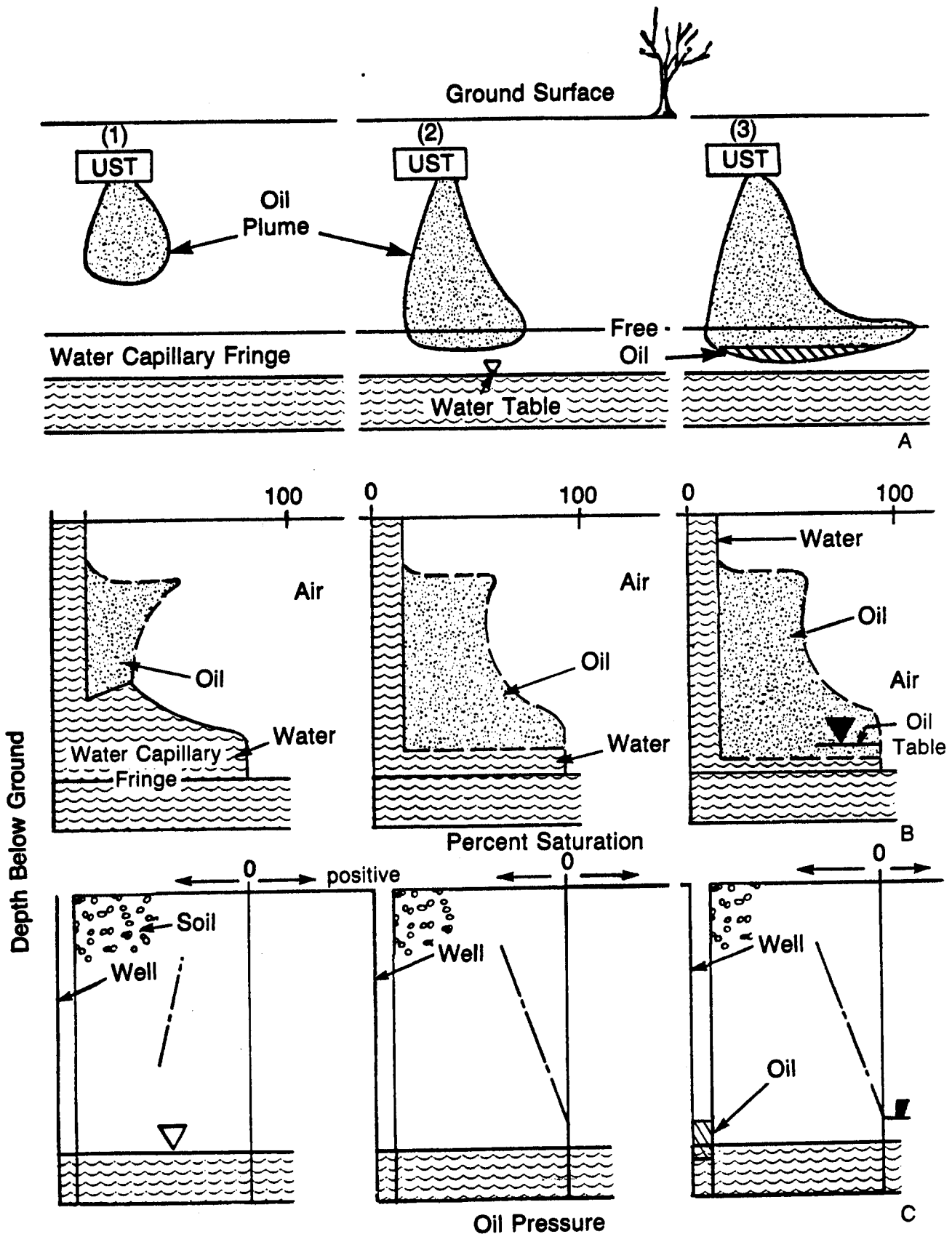
Figure 2. (A) Three stages of oil distribution in a sandy hydrogeologic system with (B) vertical profiles of percent saturation and (C) oil pressure distribution.

test the adequacy of these theoretical predictions. The results of these experiments will be presented in subsequent sections.

Quantification of Oil by Monitoring Wells

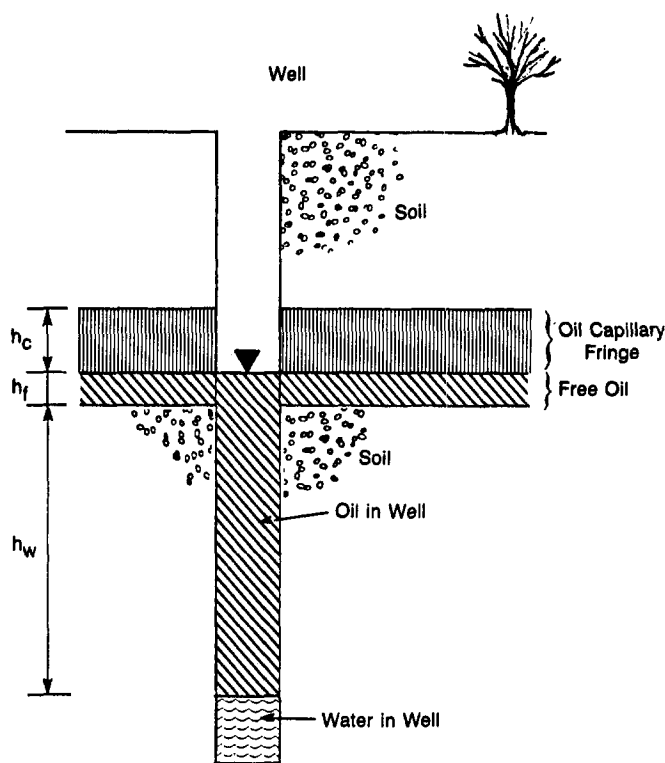It has been previously shown (CONCAWE 1979, Zilliox and Muntzer 1975) that, under hydrostatic conditions,

Figure 3. Oil distribution in a well and contiguous hydrogeologic system.

Figure 4. Water content-pressure head curves for 125 to 250 μm sand, showing the capillary fringe (CF).

the ratio of the thickness of the oil column in a well to that in the porous medium is a constant for a given oil and porous medium. This finding can be developed from Figure 3, which shows a monitoring well placed through an oil-contaminated porous medium. In this figure, h_c represents the thickness of the oil capillary fringe, h_w the thickness of the oil column in the well below the base of the free oil in the medium, and h_f the thickness of the free-oil zone in the porous medium. From Equation 3 and for a situation where h_f is very small, the following equations can be developed:

$$h_c = \frac{p_c^{oa}}{(\rho_o - \rho_a)\,g} \tag{4}$$

$$h_w = \frac{p_c^{wo}}{(\rho_w - \rho_o)\,g} \tag{5}$$

$$\frac{h_w}{h_c} = \frac{p_c^{wo}}{p_c^{oa}}\,\frac{\rho_o}{(\rho_w - \rho_o)} \tag{6}$$

where the symbols a, o, and w denote air, oil, and water, respectively.

By Equation 6, as the specific gravity of oil increases, its thickness in a monitoring well would increase with respect to that in the porous medium. For a specific gravity of 0.8 and assuming that $p_c^{wo} = p_c^{oa}$, the thickness of the oil layer in the well would be four times that in the medium. For this reason, it is sometimes assumed that the oil-thickness ratio is a constant value of four. However, this value of oil-thickness ratio may be in error during the leaking of a tank, when the value of h_f is not zero.

Knowledge of the value of h_f is very important when planning remedial schemes because it represents the volume of oil that can be readily removed from the
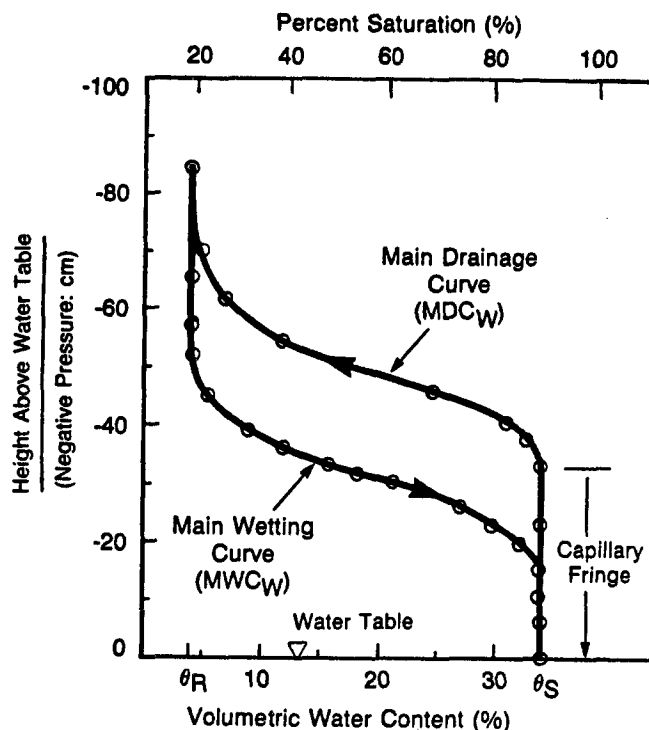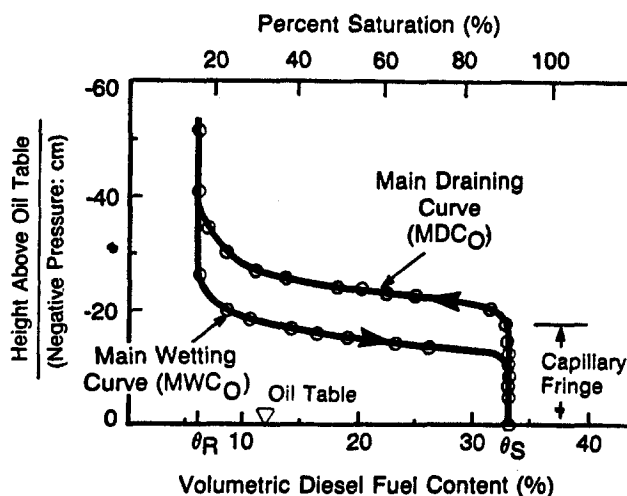

Figure 5. Diesel fuel content-pressure head curves for 125 to 250 μm sand, showing the capillary fringe (CF).

porous medium. However, estimating the value of h_f continues to be a scientific challenge (as discussed in the Results section). In addition, as the value of h_f increases, the oil thickness ratio $[(h_w + h_f)/(h_c + h_f)]$ would decrease. Therefore, the oil in the soil/aquifer system can be under-estimated if it is assumed that the oil-thickness ratio is a constant value of four. Again, these theoretical predictions will be compared with experimental findings in a subsequent section.

Experimental
Materials
The sand material used as the geologic medium in the experiments was from the water-table region of a sandy aquifer at Borden, Ontario, Canada (Abdul and Gibson 1986). The sand was first air dried and then the 125 to 250

μm (0.0049 to 0.0098-inch) grain-size range was separated, using a mechanical shaker, for use in the experiments.

Several fluids, including gasoline, kerosene, diesel fuel, transmission oil, and lubricating oils are lighter than and immiscible with water, and are of interest because they all are stored in large quantities in USTs. Diesel fuel (hereafter referred to as oil) was used in this study as a representative of the other fluids because it is less flammable than gasoline and kerosene, and therefore safer to work with. Diesel fuel also has a moderate viscosity, which helps to minimize the duration of the experiment.

The water content-pressure head $(\theta(\psi)_w)$ and oil content-pressure head $(\theta(\psi)_o)$ relationships for the sand were determined by the hanging water column method (Abdul and Gillham 1984, Day et al. 1967). The results from these funnel experiments are shown in Figures 4 and 5, respectively.

Column

The acrylic column used in the experiment was 113.5cm (44.69 inch) high by 10.8cm (4.25 inch) in diameter and was fitted at the base with a stainless steel screen and an adjustable outflow tube (Figure 6). Seven tensiometers, T1 through T7, were fitted through the wall of the column to penetrate about 1cm into the sand. Each tensiometer had a fluid chamber and two ports—a measuring port connected to a manometer and a port for flushing entrapped air from the monitoring system. The fluid chamber was separated from the sand by an 80 μm (0.0031 inch) nylon membrane. This membrane size was selected because it remained saturated with either oil or water under the range of suction in the experiment, and also because it allowed for the displacement of water by oil as the oil pressure head became positive. The monitoring well (a semicylindrical 2.5cm (0.98 inch) I.D. acrylic tube) was attached by epoxy to the outside of the length of the sand column. The wall between the well and the column was perforated with 0.6cm (0.24 inch) diameter holes and was screened from the sand medium with 125 μm (0.0049 inch) stainless-steel mesh. The column was slowly packed by pouring a continuous thin stream of sand through a funnel to achieve a uniform porous medium. The column was then tapped on the sides to compact the sand to the same bulk density ($\approx$1690 kg/m^3; 105.5 lb/ft^3) as that in the funnel experiments. After packing, the sand was slowly wetted from below until water ponded on the surface.

Experiments

In preparation for an experiment, the outflow tube (Figure 6) was positioned at the elevation of the desired initial water table and was then opened to drain the system until equilibrium was reached. Subsequently, oil slugs of 50cc (3.05 cu. inch) were added to the center of the top of the sand column at 24-hour intervals. This time interval was found to be sufficient for the system to reach equilibrium. At the end of each interval, the manometers (at T1 through T7) were monitored and the vertical distributions of oil in the column and in the well were measured. To improve the visual contrast between the oil and water in the sand medium, a few drops of a dye
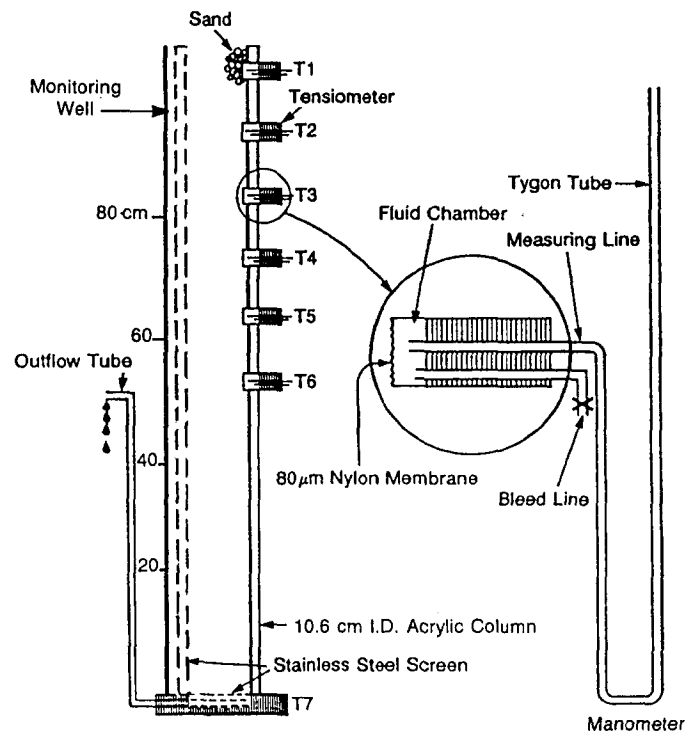
Figure 6. Schematic showing a cross section through the column, monitoring well, and tensiometer-manometer monitoring system.

(Ethyl Corp., Baton Rouge, Louisiana—an oil-soluble anthraquinone dye in an aromatic solvent) were added to the oil. All experiments were carried out under rising water-table conditions. In these experiments, the outflow tube was closed as the oil-water interface approached the top of the water capillary fringe. Under this condition, the water table and capillary fringe response to the infiltrating oil could cause the water table to rise (Abdul 1987). Experiments under falling water-table conditions, which would require drainage of displaced water from the column, were not conducted because, with the outflow tube at the base of the column opened, oil would preferentially flow through the column rather than to the well. In addition, it is not believed that such experiments would add any new insight to the problem (see Abdul 1987).

Results and Discussion

Five sets of results for critical stages during a rising water-table experiment are shown in Figures 7a through 7e. Each figure shows the well and contiguous sand medium, the oil and water distributions in the well and sand medium, and the vertical pressure head profile through the oil and water. To show the fluid distribution through the column, a unit vertical section is considered and the oil and water capillary fringes and the free-oil zone are represented by the hatched regions of this vertical section. Below the hatched region the medium is saturated with water, while above this region the medium is unsaturated with either water or oil. The measured values of pressure head are shown as closed circles connected by straight lines.

Figure 7a shows the vertical profile of the pore-water pressure, as measured at tensiometers T1 through T7, before oil was added to the top of the sand column. The bubbling pressure of the porous membrane of T1 was exceeded during the experiment and air entered the
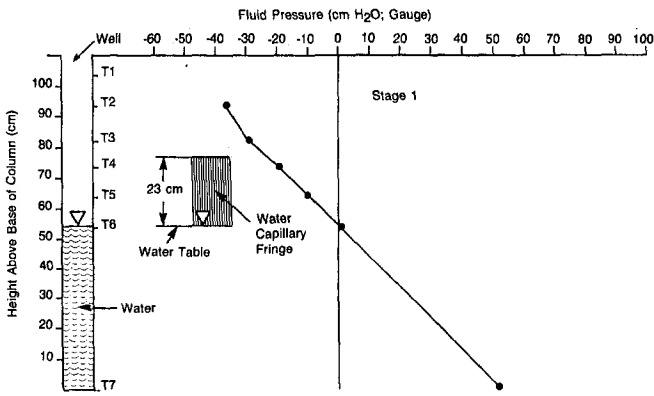
Figure 7a. Vertical profile of the pore-water pressure in the column before addition of oil.
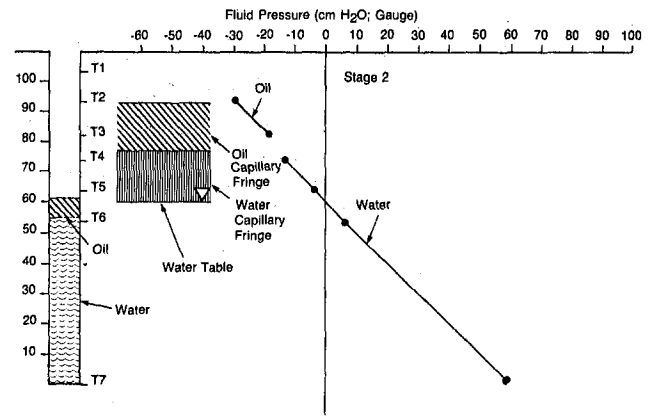

Figure 7b. Hydrostatic distribution of fluid pressure and oil-water distribution in the well and column after the oil-capillary fringe developed in the medium.
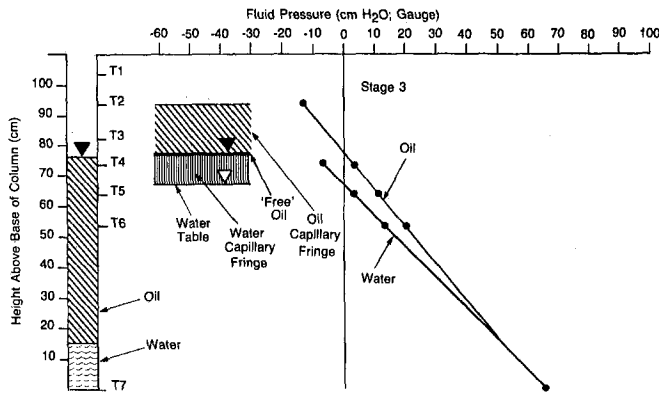

Figure 7c. Hydrostatic distribution of fluid pressure and oil-water distribution in the well and column after a layer of "free" oil developed in the medium.
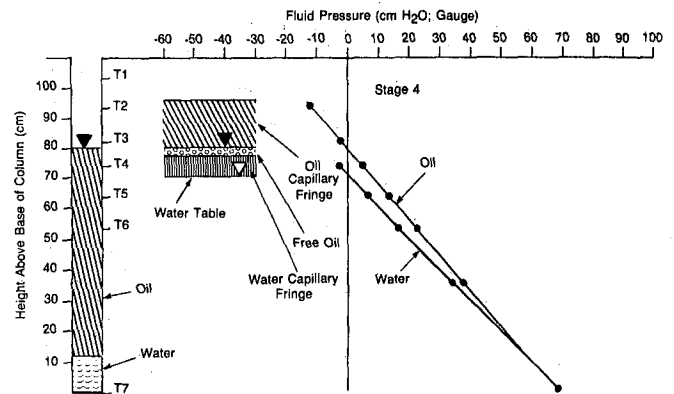

Figure 7d. Hydrostatic distribution of fluid pressure and oil-water distribution in the well and column.
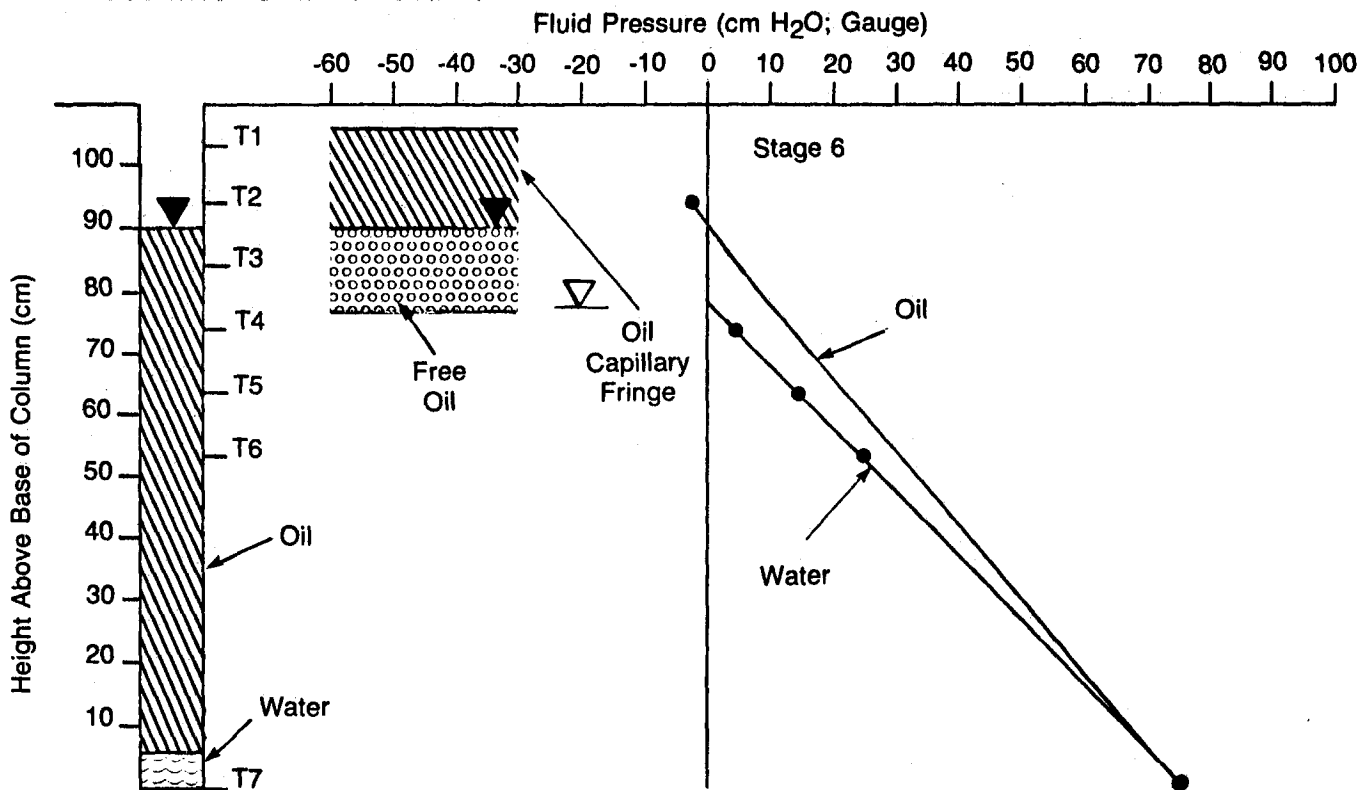

Figure 7e. Hydrostatic distribution of fluid pressure and oil-water distribution in the well and column after the water capillary fringe disappeared.

manometer line; therefore, T1 was not monitored. As expected, the results show that the pressure of the pore water increased linearly with depth below the surface of the sand (Figure 7a), indicating that the pore water was under hydrostatic conditions prior to the addition of oil. The visual thickness of the water capillary fringe in the sand column was 23cm (9.06 inch), which compares with a thickness of 33cm (12.99 inch) measured in the funnel experiments (Figure 4). This difference in the thickness of the capillary fringe is likely caused by small differences between the pore-size distribution in the funnel and column.

Figure 7b shows the conditions in the column when the oil capillary fringe was fully developed and oil began to flow into the well. During the development of the fringe, no oil flowed into the well. Only after the development of a saturated oil fringe did the excess oil start to drain into the well. At this stage of the experiment, the volume of excess oil was smaller than that needed to cause the oil in the well to rise to the level of the base of the oil capillary fringe in the medium. Under this condition, no free-oil layer existed in the medium ($h_f = 0$). As more oil was added, the excess oil in the medium drained into the well causing the oil/air interface in the well to rise to the level of the base of the oil capillary fringe in the medium and forcing the oil-water interface in the well to fall (Figure 7c). At this stage, a thin layer of free oil accumulated in the medium. Further addition of oil caused the oil/air interface and oil/water interface in the well to rise and fall, respectively. The thickness of the free-oil layer increased and the water table rose as a result of the water capillary fringe decreasing in thickness (Figures 7d and 7e). Because the response of the water capillary fringe will determine the final position of the water table, a detailed treatment of its response is described elsewhere in this paper.

The vertical distribution of the hydrostatic pressure through the oil in the sand column and in the well and the hydrostatic pressure through the water in the sand column can be described by two straight lines (Figures 7c to 7e). The pressures of the oil and water in the medium at the plane passing through the oil-water interface in the well are equal, indicating that the pressure exerted by the oil column in the well is balanced by the pressure of the water column in the contiguous porous medium. Above this plane, the two pressure lines (one for water and the other for oil) diverge such that the pressure in the oil is always higher than that in the water. The maximum difference between the oil and water pressures is reached at the elevation of the oil-water interface in the porous medium. This is the pressure that the oil must exceed relative to that of water to displace water from the saturated pores of the sand.

The results in Figure 7 also show that the visual observations are in excellent agreement with the measured hydrostatic pressure-head distributions. The intersection of the oil-pressure line and the vertical zero-pressure line (the oil table) is at the same height above the base of the column as the observed top of the oil column in the well. In addition, the pressure of the column of water between the measured water-table position and the oil-water interface in the well matches the pressure of the visually observed oil column in the well. Some of the results in Figure 7 are summarized in Table 1 for further discussion.

Oil-Thickness Ratio

The oil-thickness ratio (R) is defined here as the ratio of the oil thickness in the well (H_{ow}) to that in the adjacent porous medium (H_{om}). Recall that H_{om} is the sum of the height of the oil capillary fringe ($h_c = 16cm$ [6.30 inch] in the column; 23cm [9.06 inch] in funnel) and the thickness of the free-oil zone (h_f), while H_{ow} is the sum of h_f and the thickness of oil in the well below the base of oil in the porous medium (h_w) (Figure 3).

The experimental results demonstrated that oil would enter a well only after a zone of free product (oil pressure above atmospheric pressure) starts to develop (Figure 7b). Just prior to the development of the zone of free product, the value of H_{om} was equivalent to the thickness

TABLE 1
Summary of Experimental Results

Figure	$(h_w + h_f)$ (cm)	$(h_c + h_f)$ (cm)	R	WCF (cm)	p_c^{wo} (cm H_2O)	H_f (cm)
7B	6	16	0.4	17	—	—
7C	63	17	3.7	9	9	1
7D	68	19	3.6	6.5	9.5	3
8	73	23	3.2	2	9	7
7E	84	29	2.9	0	11.5	13

$(h_w + h_f)$ ≡ thickness of oil in the well.
$(h_c + h_f)$ ≡ thickness of oil in the porous medium.
WCF ≡ thickness of the water capillary fringe.
p_c^{wo} ≡ pressure difference across the oil-water surface.
h_f ≡ thickness of free product in the porous medium.
R ≡ $(h_w + h_f)/(h_c + h_f)$

of the oil capillary fringe, while the value of H_{ow} was zero. As the zone of free product developed and oil entered the well, the oil thickness ratio increased from zero to a value of 3.6 (Figure 7d), while the value of h_f remained quite small (Table 1). Subsequently, as h_f increased to 13cm (5.12 inch), the value of R decreased to 2.9 (Figure 7e). During the experiment, the thickness of the oil capillary fringe remained constant; therefore, the decrease in the values of R resulted from the corresponding increase in the values of h_f. These results clearly demonstrate that the oil-thickness ratio, for the same medium and oil, is not a constant but that it first increases to a maximum value and then decreases as the thickness of free oil increases from zero.

Based on these results, estimates of the oil thickness in the porous medium from the measured thickness of the oil column in a monitoring well under the assumption that the value of R is constant may be in error. The greatest challenge in estimating the value of R is in locating the oil-water interface in the porous medium. Under hydrostatic conditions, this interface is located at the elevation at which the pressure difference between the oil-and water-pressure lines is equal to the interfacial pressure between oil and water (Equation 2). In an effort to find a simple procedure to give reasonable estimates of R we will: (1) use the measurements in the monitoring well for an advanced stage during the experiment (Figure 8) to construct the oil and water pressure lines; (2) calculate, for hydrostatic conditions, the capillary pressure at the oil-water interface using results of simple laboratory funnel experiments and Equation 2; and (3) find the elevation of

this pressure difference between the oil- and water-pressure lines. The agreement between the calculated and observed thickness of the oil in the sand column will be assessed.

Because the volume of the monitoring well (in the laboratory experiment and also in field applications) is very small, the top of the oil column in the well was at the same elevation as the base of the oil capillary fringe in the adjacent porous medium (point A, Figure 8). Under hydrostatic conditions, the oil pressure at the oil-water interface in the well would be equal to the pore-water pressure in the adjacent porous medium (point B, Figure 8). A straight line through the points A and B, which were located from observation in the monitoring wells (measurements in field applications) describes the hydrostatic pressure profile for the oil in the contiguous porous medium and well. Further, the position of the water table in the porous medium is determined by the water head that is required to support the column of oil in the well, and is the product of the measured oil thickness in the well and the ratio of the densities of oil and water (point C, Figure 8). The equilibrium pressure profiles calculated from the measurements made in the monitoring well are shown by broken lines in Figure 8, while the pressure profiles determined from the manometers are indicated by solid lines. Next we will locate the oil-water interface in the porous medium and compare the calculated position with that observed experimentally.

Under hydrostatic conditions the pressure head in the oil would be such that oil cannot displace water and the pressure across the oil-water interface in the porous medium can be calculated by using Equation 3. Using the
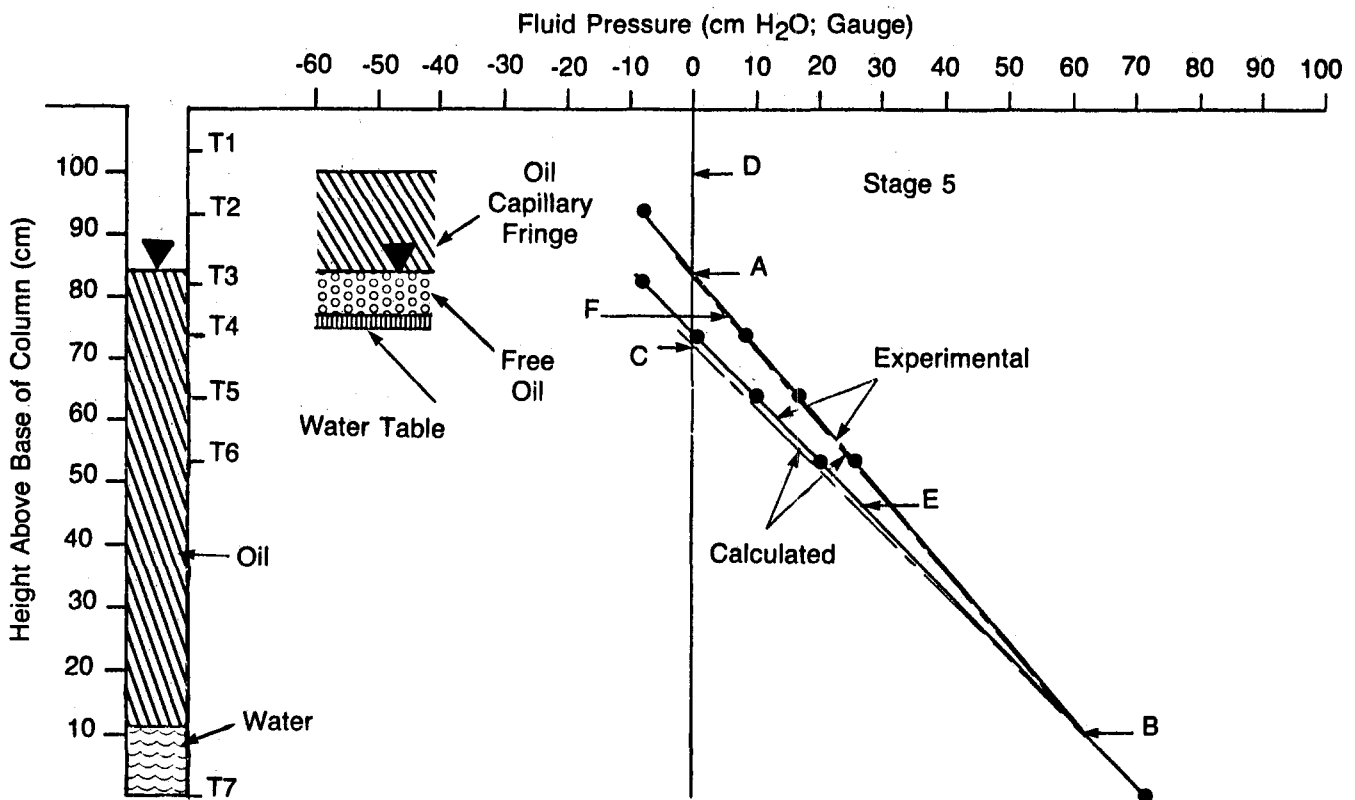

Figure 8. Hydrostatic distribution of measured and calculated fluid pressure and oil-water distribution in the well and column. For a stage in the experiment between the conditions in Figures 7d and 7e.

heights of the oil- and water-capillary fringe (h_c), measured in the funnel and column experiments, two values for p_c^{wa} and for p_c^{oa} were calculated.

These values, with corresponding values of surface tension for air-water and air-oil ($\simeq$75 dynes/cm [0.014 poundals/inch] and $\simeq$32 dynes/cm [0.059 poundals/inch], respectively), and a contact angle of zero were used with Equation 2 to calculate four values of r_{eff} (0.0069, 0.0049, 0.0048, and 0.0046cm [0.0027, 0.0019, 0.0019, and 0.0018 inch]) for the column sand. The mean value of r_{eff} is 0.0053cm (0.0021 inch). Further, for this value of mean r_{eff}, a mean laboratory-measured value for the interfacial tension between oil and water of 15.5 dynes/cm (0.0028 poundals/inch), and cos $\theta = 1$, Equation 2 gives a value of p_c^{wo} of 6.0cm water (2.36 inch). By this calculation the base of the oil zone in the porous medium should be the elevation at which the pressure difference between the oil pressure line (BA) and the water pressure line (BC) is 6.0cm (2.36 inch). This corresponds to elevation E in Figure 8. The observed position of the oil-water interface in the column experiment corresponds to a value of p_c^{wo} of 9cm (3.54 inch) water (position F in Figure 8). The difference in elevations at E and F represents a difference of 30cm (11.81 inch) oil. Based on this calculation, the thickness of the zone of free oil in the sand is 37cm (14.57 inch) compared to the observed thickness of 7cm (2.76 inch). This difference is of practical significance because a free-oil-zone thickness of a few centimeters represents a large volume of oil if the lateral spread is large.

The values of p_c^{wo} for the several stages of the experiment are included in Table 1 and they range from 9.0 to 11.5 (cm water). Because the value p_c^{wo} used in the preceding calculations is 9.0 (cm water), the foregoing analysis is applicable to all the results of this study. This analysis demonstrates that even in the well-controlled experiment with an adequately characterized sand column, the calculated position of the oil-water interface in the porous medium can be significantly different from the actual position of this interface. At field sites, where locating the interface currently relies on measurements in monitoring wells, predictions of the value of R can be expected to be much more uncertain due to a dynamic flow system and spatial variability of the hydrogeologic parameters.

A simple and direct method for measuring the mean height of the oil- and water-capillary fringe (Abdul and Gillham 1984) gave results that show some dependence on the size of the laboratory device. In the column, the volume of sand was about 85 times that in the funnel cell, and the vertical extents for the oil- and water-capillary fringes were 16 and 23cm (6.30 and 9.06 inch), while in the funnel they increased to 18 and 33cm (7.09 and 12.99 inch), respectively. This difference in the vertical extent of the capillary fringe is likely caused by small differences in the values of bulk density in the funnel and column.

Response of Water Table and Capillary Fringe

At the start of the experiment, the vertical extent of the water-capillary fringe was 23cm (9.06 inch) and the tops of the fringe and the water table were at heights of 77 (30.31 inch) and 54cm (21.26 inch) from the bottom of the
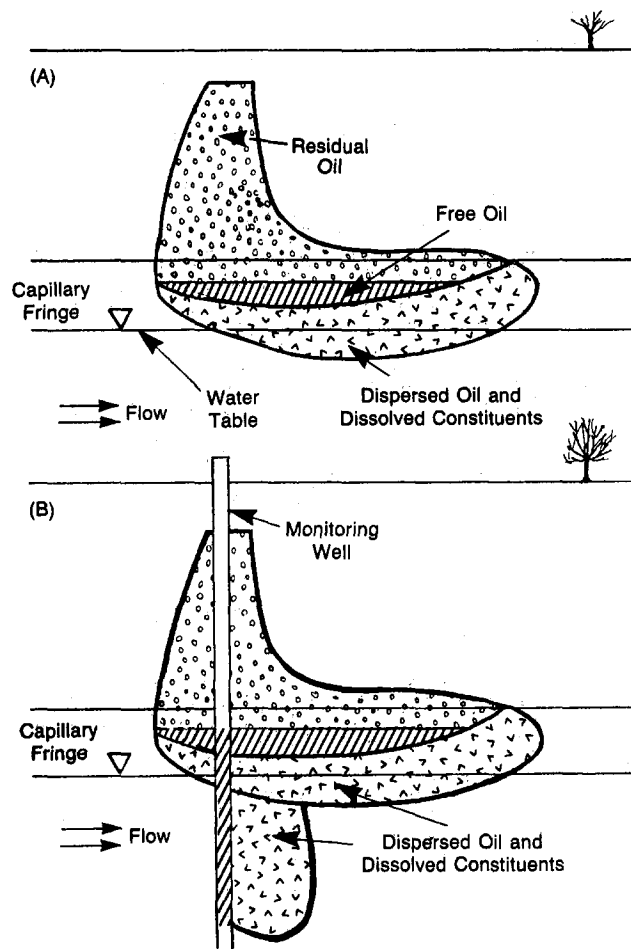
Figure 9. Plumes of oil and oil constituents: (A) before and (B) after installation of monitoring well.

column, respectively (Figure 7a). The oil-water interface, once formed at the top of the capillary fringe, remained at that elevation throughout the experiment (Figures 7b to 7e). However, the vertical extent of the water capillary fringe decreased from 23 to 0cm (9.06 to 0 inch) during the experiment due to a rising water table. The initial rise in the water table was likely caused by small quantities of water displaced by oil from the lower region of the funicular zone after the outflow tube was closed. This contribution is not believed to be significant in view of the fact that the oil-water interface was initially formed at the top of the water capillary fringe. However, the water-table rise and the decrease in the thickness of the capillary fringe (see Table 1) occurred in response to a corresponding increase in the oil head in the medium. At each stage in the experiment, the increase in the thickness of the oil in the well is balanced by a rise in the water table.

These experimental observations have provided some insights into potential responses of the capillary fringe and water table under an active leak. However, factors such as the rate of leak, fluctuating water-table conditions, and spatial variation in the hydrogeologic conditions at the site could significantly influence the response of the system to the oil leak.

Enhanced Aquifer Contamination

A typical schematic for oil distribution in a homogeneous sandy aquifer is shown in Figure 9a (Schwille

1967, Schwille 1984, Abdul 1987). The free-oil zone takes the shape of a "pancake" having a small vertical extent compared to its horizontal extent. For small leaks, the hydrocarbon source for potential aquifer contamination is along the oil-water interface in the water capillary fringe.

When a monitoring well is placed through the zone of free oil, enhanced vertical contamination can occur during drilling. In addition, because oil in the monitoring well can fall several feet below the base of the pancake, the oil column in the well can provide a vertical source of contaminants (Figure 9b). Such vertical spread would be enhanced by fluctuations of the water table.

Careful determination of the depths of coring, drilling, and well installation would minimize the potential of further spreading the contaminants by these activities.

Conclusion

Monitoring wells are routinely used to detect petroleum products leaking from underground storage tanks and to delineate the zones of soil and aquifer systems contaminated by these products. Also, measurements in monitoring wells are often used to estimate the amount of product in the contaminated soil/aquifer system. Both theoretical analysis and laboratory column experiments with sandy aquifer material and diesel fuel have shown that monitoring wells alone are not adequate for the aforementioned applications.

Acknowledgments

Biographical Sketches

Abdul S. Abdul received his Ph.D. in contaminant hydrogeology from the Institute of Ground Water Research, Department of Earth Sciences, University of Waterloo in 1985. He has been a member of the Environmental Science Department in General Motors Research Laboratories (Warren, MI 48090-9055) since 1985. His major interests include the movement of immiscible fluids and reactive solutes through hydrogeologic materials, and the development of technologies based on physical, chemical, and biological processes to clean up contaminated soil and aquifer systems.

Thomas L. Gibson received his Ph.D. in chemistry from the University of Texas at Austin in 1972. A professional staff member of the Environmental Science Department in General Motors Research Laboratories (Warren, MI 48090-9055) since 1979, his primary research interests are in the investigation and remediation of toxic contaminants in the environment. Dr. Gibson is a member of the American Chemical Society, the American Geophysical Union, and the Association of Ground Water Scientists and Engineers. His research has included publications in areas of contaminant migration through hydrogeologic systems, measurement of toxic and mutagenic pollutants, and atmospheric chemistry.

Sheila F. Kia is a staff research engineer in the Department of Environmental Science at the General Motors Research Laboratories (Warren, MI 48090-9055). She received a Ph.D. from Cambridge University and pursued post-doctoral research at the University of Michigan, Ann Arbor. Her current research interests include multiphase flow of immiscible fluids, physical processes and heterogeneities in porous media, contaminant recovery, and colloidal chemistry.

References

Abdul, A.S. 1988. Migration of petroleum products through sandy hydrogeologic systems. *Ground Water Monitoring Review*, vol. 8, no. 4, p. 73.

Abdul, A.S., and T.L. Gibson. 1986. Equilibrium batch experiments with six polycyclic aromatic hydrocarbons by two aquifer materials. *Hazardous Waste and Hazardous Materials*, vol. 3, no. 2, p. 125.

Abdul, A.S., and R.W. Gillham. 1984. Laboratory studies of the effects of the capillary fringe on streamflow generation. *Water Resour. Res.*, vol. 20, no. 6, p. 691.

CONCAWE. 1979. Protection of groundwater from oil pollution. CONCAWE Rep. No. 3/79, The Hague.

Corey, A.T. 1977. Mechanics of heterogeneous fluids in porous media. Water Resour. Publ., Fort Collins, Colorado.

Day, P.R., G.H. Bolt, and D.M. Anderson. 1967. Nature of soil water, *Irrigation and Agricultural Lands*. Eds. R.M. Hagan, H.R. Haise, and T.W. Edminster, American Soc. of Agronomy, Madison, Wisconsin, Agronomy 9, pp. 193-208.

Dullien, F.A. 1979. *Porous Media Fluid Transport and Pore Structure*. Academic Press, New York.

Schwille, F. 1967. Petroleum contamination of the subsoil: A hydrological problem in the joint problems of the oil and water industries. Ed. P. Hepple, The Institute of Petroleum, London, p. 23.

Schwille, F. 1984. Migration of organic fluids immiscible with water in the unsaturated zone. In *Pollutants in Porous Media*, B. Yaran, D. Dagan, J. Goldshmid, Eds. Springer-Verlag, New York.

Zilliox, L., and P. Muntzer. 1975. Effect of hydrodynamic processes on the development of groundwater pollution. *Progress in Water Technology*, vol. 7, p. 561.